The current issue and full text archive of this journal is available at
www.emeraldinsight.com/0961-5539.htm

Thermal-fluid flow within innovative heat storage concrete systems for solar power plants

Valentina A. Salomoni and Carmelo E. Majorana
Department of Construction and Transportation Engineering, Faculty of Engineering, University of Padua, Padua, Italy, and
Giuseppe M. Giannuzzi and Adio Miliozzi
ENEA – Agency for New Technologies, Energy and Environment, Thermodynamic Solar Project, CRE Casaccia, Rome, Italy

Received 28 March 2007
Revised 31 July 2007
Accepted 8 November 2007

Abstract

Purpose – The purpose of this paper is to describe an experience of R&D in the field of new technologies for solar energy exploitation within the Italian context. Concentrated solar power systems operating in the field of medium temperatures are the main research objectives, directed towards the development of a new and low-cost technology to concentrate the direct radiation and efficiently convert solar energy into high-temperature heat.

Design/methodology/approach – A multi-tank sensible-heat storage system is proposed for storing thermal energy, with a two-tanks molten salt system. In the present paper, the typology of a below-grade cone shape storage is taken up, in combination with nitrate molten salts at 565°C maximum temperature, using an innovative high-performance concrete for structures absolving functions of containment and foundation.

Findings – Concrete durability in terms of prolonged thermal loads is assessed. The interaction between the hot tank and the surrounding environment (ground) is considered. The developed FE model simulates the whole domain, and a fixed heat source of 100°C is assigned to the internal concrete surface. The development of the thermal and hygral fronts within the tank thickness are analysed and results discussed for long-term scenarios.

Originality/value – Within the medium temperature field, an innovative approach is here presented for the conceptual design of liquid salts concrete storage systems. The adopted numerical model accounts for the strong coupling among moisture and heat transfer and the mechanical field. The basic mathematical model is a single fluid phase non-linear diffusion one based on the theory by Bažant; appropriate thermodynamic and constitutive relationships are supplemented to enhance the approach and catch the effects of different fluid phases (liquid plus gas).

Keywords Solar power, Concretes, Flow, Thermal insulating properties

Paper type Research paper

Introduction

Energy availability has always been an essential component of human civilization and the energetic consumption is directly linked to the produced wealth. In many depressed countries the level of solar radiation is considerably high and it could be the primary energy source, under conditions that low cost, simple-to-be-used technologies are employed. Then, it is responsibility of the most advanced countries to develop new equipments to allows this progress for taking place. A large part of the energetic forecast, based on economic projection for the next decades, ensure us that fossil fuel

International Journal of Numerical Methods for Heat & Fluid Flow
Vol. 18 No. 7/8, 2008
pp. 969-999

0961-5539
DOI 10.1108/09615530810899051

supplies will be largely enough to cover the demand. The predicted and consistent increase in the energetic demand will be more and more covered by a larger use of fossil fuels, without great technology innovations. A series of worrying consequences are involved in the above scenario: important climatic changes are linked to strong CO_2 emissions; sustainable development is hindered by some problems linked to certainty of oil and natural gas supply; problems of global poverty are not solved but amplified by the unavoidable increase in fossil fuel prices caused by an increase in demand.

These negative aspects can be avoided only if a really innovative and more acceptable technology will be available in the next decades at a suitable level to impress a substantial effect on the society. Solar energy is the ideal candidate to break this vicious circle between economic progress and consequent greenhouse effect. The low penetration on the market shown today by the existent renewable technologies, solar energy included, is explained by well-known reasons: the still high costs of the produced energy and the "discontinuity" of both solar and wind energies. These limitations must be removed in reasonable short times, with the support of innovative technologies, in view of such an urgent scenario.

On this purpose ENEA, on the basis of the Italian law no. 388/2000, has started an R&D program addressed to the development of concentrated solar power (CSP) systems able to take advantage of solar energy as heat source at high temperature. One of the most relevant objectives of this research program (Rubbia, C., and ENEA Working Group, 2001) is the study of CSP systems operating in the field of medium temperatures (about 550°C), directed towards the development of a new and low-cost technology to concentrate the direct radiation and efficiently convert solar energy into high-temperature heat; another aspect is focused on the production of hydrogen by means of thermo-chemical processes at temperatures above 800°C.

The problems concerning the use of CSP technologies has been analyzed and reported by several authors, e.g. Sargent & Lundy Consulting Group (2002) conclude that the CSP technology is a well-established and reliable solution for energy production, even if its major disadvantage is that the energy produced is at much higher costs than those required by fossil-fuels. The authors propose to enlarge the market of such technologies and increase their use, thus reducing costs. Price *et al.* (2002) discuss how a torque box design for parabolic trough collectors, an important aspect in concentrating solar thermal power plants in California, reduces weight and deformations of collector structures. Reducing weight and deformations will subsequently decrease the number of drives and interconnecting pipes hence allowing for more collector elements onto one drive. By using this design of parabolic trough collector, the potential for very large costs reductions comes out. Lüpfert *et al.* (2001) consider how the existing parabolic trough power plants are a capable and ever-growing technology and, thanks to improvements reached through R&D, it is likely that costs will consistently decrease while advantages and technology rapidly increase.

As well as cost reductions, the current innovative ENEA conception aims to introduce a set of innovations, concerning:

- *The parabolic-trough solar collector.* An innovative design to reduce production costs, installation and maintenance and to improve thermal efficiency is defined in collaboration with some Italian industries.

- *The heat transfer fluid.* The synthetic hydrocarbon oil, which is flammable, expensive and unusable beyond 400°C, is substituted by a mixture of molten salts (sodium and potassium nitrate), widely used in the industrial field and chemically stable up to 600°C.
- *The thermal energy storage (TES).* It allows for the storage of solar energy, which is then used when energy is not directly available from the sun (night and covered sky) (Pilkington Solar International GmbH, 2000).

After some years of R&D activities, ENEA has built an experimental facility (defined within the Italian context as *Prova Collettori Solari* – PCS) at the Research Centre of Casaccia in Rome (ENEA, 2007), which incorporates the main proposed innovative elements (Figure 1).

The next step is to test these innovations at full scale by means of a demonstration plant, as envisioned by the "Archimede" ENEA/ENEL project in Sicily. Such a project is designed to upgrade the ENEL thermo-electrical combined-cycle power plant by about 20 MW, using solar thermal energy from concentrating parabolic-trough collectors.

Point (1) above is being analysed today by the authors (Giannuzzi *et al.*, 2007) and first design criteria are being suggested, whereas the attention now is focused on point (3) already introduced in (Giannuzzi *et al.*, 2005), as explained in the following.

Two-tanks CSP systems

The main advantage of thermal solar power plants is the possibility to use relatively economical storage systems, if compared to other renewable energies (i.e. photo-voltaic and wind). Storing electricity is much more expensive than storing thermal energy itself. TES option can collect energy in order to shift its use to later times, or to smooth out the plant output during irregularly cloudy weather conditions. Hence, the functional operativeness of a solar thermal power plant can be extended beyond periods of no solar radiation without the need of burning fossil fuel. Periods of mismatch among energy supplied by the sun and energy demand can be reduced.

Figure 1.
PCS tool solar collectors at ENEA Centre (Casaccia, Rome)

Economic thermal storage is a technological key issue for the future success of solar thermal technologies.

In our days, among eight thermal storage systems in thermo-electric solar plants, seven have been of experimental or prototypal nature and only one has been a commercial unit (Table I). All the listed systems are "at sensible heat storage": two single-tanks oil thermo-cline systems, four two-tanks single medium systems (one oil- and three molten salt) and two single-tanks double medium systems. Actually the most advanced technology for heat storage in solar towers and through collector plants considers the use of a two-tanks molten salt system (Ives *et al.*, 1985).

The functional thermodynamic process of a parabolic-trough two-tanks solar plant is shown in Figure 2 (Herrmann *et al.*, 2004). The main elements of the plant are: the solar field, the storage system, the steam generator and the auxiliary systems for starting and controlling the plant.

The solar field is the heart of the plant; the solar radiation replaces the fuel of conventional plants and the solar concentrators absorb and concentrate it. The field is made up of several collector elements composed in series to create the single collector line. The collected thermal energy is determined by the total number of collector elements which are characterized by a reflecting parabolic section (the concentrator), collecting and continuously concentrating the direct solar radiation by means of a sun-tracking control system to a linear receiver located on the focus of the parabolas. A circulating fluid flows inside a linear receiver to transport the absorbed heat.

The hot and cold tanks (Figure 3) are located on the ground and they are characterized by an internal circumferential and longitudinally-wrinkled liner, appropriately thermally insulated. The cost of the liner is the primary cost of such a tank (Figure 4). In recent studies it has been shown that an increase in the hourly capacity accumulation reduces sensibly the cost of the produced electrical energy; this leads to increase the reservoir dimensions from the 11.6 m diameter and 8.5 m height of the Solar Two power plant to the larger 18.9 m diameter and 2.5 height calculated in the Solar Tres power plant design phase.

Already in 1985, the Solar Energy Research Institute (SERI) commissioned the conceptual design of a below-grade cone shape storage (Figure 5) with 900°C molten carbonate salts (Copeland *et al.*, 1984). This solution, even though interesting because of the use of low-cost structural materials, showed some limits connected to the high level of corrosion induced by carbonate and high temperature.

In this paper, such a type of storage is reconsidered in combination with nitrate molten salts at a maximum temperature of 565°C, using an innovative high-performance concrete (HPC) for the tanks. From the technological point of view, the innovations relies in:

- higher structural safety related to the reduced settlements;
- employment of HPC containment structures and foundations characterised by lower costs with respect to stainless steel structures;
- substitution of highly expensive corrugated steel liners with plane liners taking advantage of the geometric compensation of thermal dilations due to the conical shape of the tank;

Project	Type	Storage medium	Cooling loop	Nominal temperature (°C)		Storage concept	Tank volume (m^3)	Thermal capacity (MW)
				Cold	Hot			
Irrigation pump, Coolidge, AZ, USA	Parabolic trough	Oil	Oil	200	228	1 Tank Thermo-cline	114	3
IEA-SSPS, Almeria, Spain	Parabolic trough	Oil	Oil	225	295	Tank Thermo-cline	200	5
SEGS I, Dogget, CA, USA	Parabolic trough	Oil	Oil	240	307	Cold tank Hot tank	4,160 4,540	120
IEA-SSPS, Almeria, Spain	Parabolic trough	Oil Cast iron	Oil	225	295	1 Dual Medium tank	100	4
Solar One, Barstow, CA, USA	Central receiver	Oil/sand rock	Steam	224	304	1 Dual Medium tank	3,460	182
CESA-1, Almeria, Spain	Central receiver	Liquid salt	Steam	220	340	Cold tank Hot tank	200 200	12
THEMIS, Targasonne, France	Central receiver	Liquid salt	Liquid salt	250	450	Cold tank Hot tank	310 310	40
Solar Two, Barstow, CA, USA	Central receiver	Liquid salt	Liquid salt	275	565	Cold tank Hot tank	875 875	105

Table I.
Different projects for thermal storage in solar plants

- possibility of employing freezing passive systems for the concrete basement made of HPC, able to sustain temperature levels higher than those for OPC; and
- fewer problems when the tank is located on low-strength soils.

The planned research activities required the upgrade of a FE coupled model for heat and mass transport (plus mechanical balance) to estimate concrete tanks durability under prolonged thermal loads and cyclic temperature variations due to changes in the salts level. The presence of a surrounding soil volume is additionally accounted for to evaluate environmental risk scenarios.

The mathematical model

Concrete is treated as a multiphase system where the voids of the skeleton are partly filled with liquid and partly with a gas phase (Baggio *et al.*, 1995; Gawin *et al.*, 1999). The liquid phase consists of bound water (or adsorbed water), which is present in the whole range of water contents of the medium, and capillary water (or free water), which appears when water content exceeds so-called solid saturation point S_{ssp} (Couture *et al.*, 1996), i.e. the upper limit of the hygroscopic region of moisture content. The gas phase, i.e. moist air, is a mixture of dry air (non-condensable constituent) and water vapour (condensable gas), and is assumed to behave as an ideal gas.

The approach here is to start from a phenomenological model (Schrefler *et al.*, 1989; Majorana *et al.*, 1997, 1998; Majorana and Salomoni, 2004; Salomoni *et al.*, 2007), originally developed by Bažant and co-authors, e.g. (Bažant, 1975b;

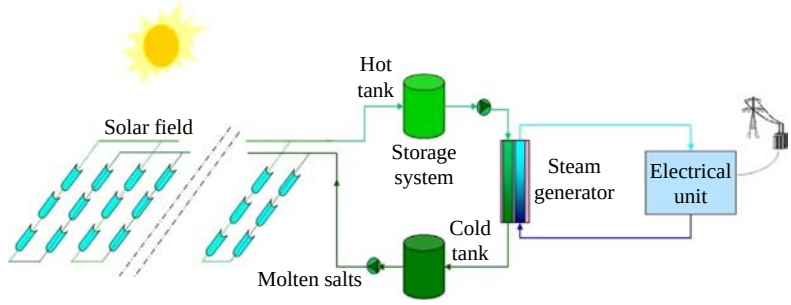

Figure 2.
Functional thermodynamic process flow of a solar plant

Figure 3.
Solar two thermal storage, steam and generator systems (Barstow, California)

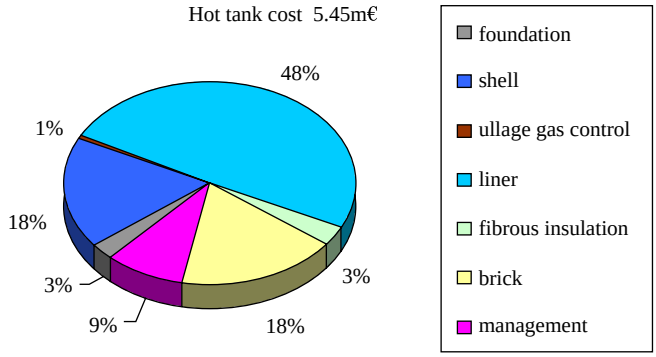

Figure 4.
Solar two thermal storage costs

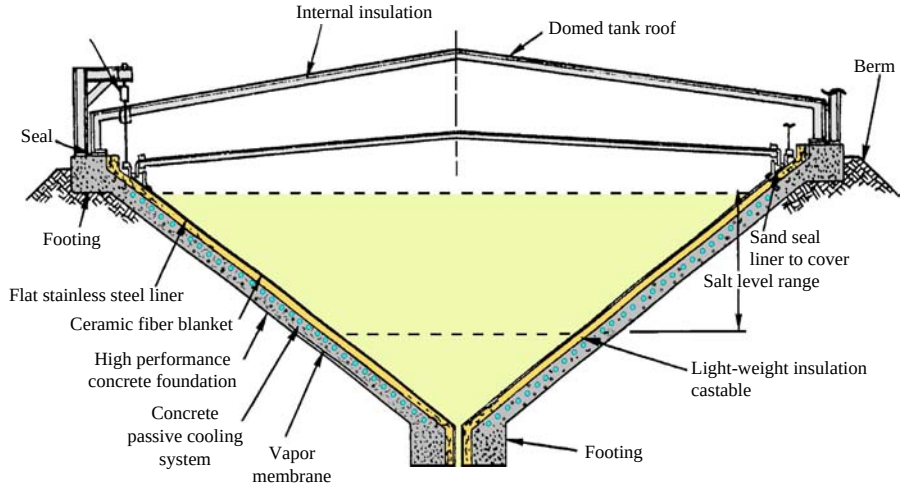

Figure 5.
Conical storage partially buried in the ground

Bažant and Thonguthai, 1978, 1979; Bažant *et al.*, 1988), in which mass diffusion and heat convection-conduction equations are written in terms of relative humidity, to an upgraded version in which its non-linear diffusive nature is maintained as well as the substitution of the linear momentum balance equations of the fluids with a constitutive equation for fluxes, but new calculations of thermodynamic properties for humid gases are implemented too to take into account different fluid phases as well as high ranges of both pressure and temperature. Additionally, Darcy's law is abandoned when describing gas flow through concrete.

The proposed model couples non-linear geometric relations with empirical relations; to enhance its predictive capabilities, a predictor-corrector (PC) procedure is supplemented to check the exactness of the solution.

Field equations for the coupled heat and moisture transfer in concrete materials

For the continuity equation, it is assumed that the various phases of water in each pore (vapour, capillary water and adsorbed water) are in thermodynamic equilibrium with each other (Bažant and Najjar, 1972) and with the solid skeleton. The relation between

h (relative humidity) and w (moisture content) at variable temperature is now:

$$dh = Kdw + kdT + dh_s - \chi \mathbf{m}^T d\varepsilon, \quad (1)$$

where $K = (\partial h/\partial w)\big|_T$ is the inverse slope of the desorption isotherm, $k = (\partial h/\partial T)\big|_{w,\varepsilon}$ is the hygrothermic coefficient representing the change in h due to 1° change of T at constant w, ϵ and a fixed degree of saturation, dh_s is the self-desiccation and $\chi = (\partial h/\partial \varepsilon_v)\big|_{T,w}$ equals the change in h due to unit change of volumetric strain ϵ_v at constant w, constant T and given degree of saturation. The last term in the right hand side of equation (1) represents the coupling term for connecting hygro-thermal and mechanical responses (Schrefler *et al.*, 1989).

The relative humidity connects the equilibrium water vapour pressure p_{gw} to the saturation pressure p_{gws} through the Kelvin equation (Gregg and Sing, 1982):

$$p_{gw} = p_{gws}(T)h, \quad (2)$$

where p_{gws} can be calculated, e.g. from Hyland and Wexler (1983) or ASHRAE (1997).

The diffusion equation governing moisture movement in concrete is known to be highly non-linear, due principally to diffusivity being strongly dependent on relative humidity (Bažant and Najjar, 1971, 1972), as shown in Figure 6. Loss of moisture must therefore be treated as a non-linear diffusion problem, and since humidity change really depends on the free energy of water, a basic equation is (Bažant, 1988):

$$\mathbf{J} = C\,\mathrm{grad}\,\mu_w, \quad (3a)$$

where μ_w is the free energy of water; C, the diffusivity, can be expressed as:

$$C = aK \quad (3b)$$

and a is the permeability, function of both h and T (see below).

Additionally, the relation between the rate of change of the mass of water per unit volume and the flux field is defined by:

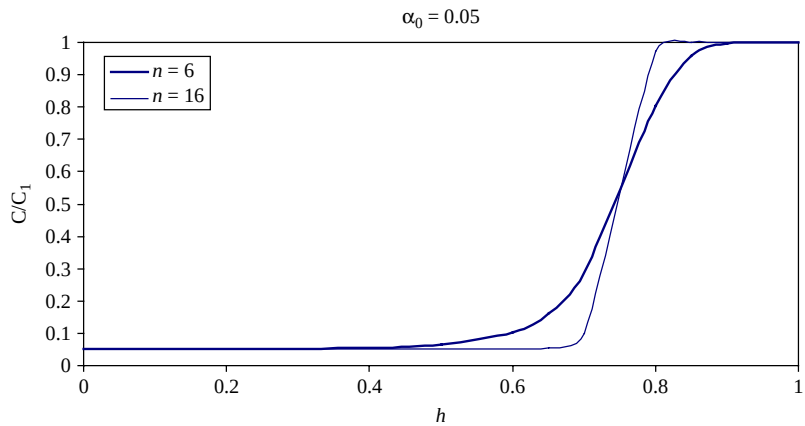

Source: Redrawn from Bazant and Najjar (1971)

Figure 6.
Variation of the diffusion coefficient with relative humidity, equations (5a)-(5c)

$$\frac{\partial w}{\partial t} = -\mathrm{div}\mathbf{J}. \tag{4}$$

Bažant and Najjar (1972) used the following expression:

$$C(h) = C_1\left[\alpha_0 + \frac{1-\alpha_0}{1+(1-h/1-h_c)^n}\right], \tag{5a}$$

in which $h_c = 0.75$, $6 \le n \le 16$, $0.025 \le \alpha_0 \le 0.10$, and C_1 is given by:

$$C_1 = C_{10}\left(1+\frac{10}{t_e}\right) \quad (t_e \text{ in days}), \tag{5b}$$

where C_{10} is a material constant and t_e is an equivalent time.

In Bažant (1986), the following expression for C_1 is suggested:

$$C_1(T, t_e) = C_0\left[0.3+\sqrt{\frac{13}{t_e}}\right]\frac{T}{T_0}e^{(Q/R)((1/T_0)-(1/T))}, \tag{5c}$$

in which C_0 is the diffusivity at 28 days and temperature T_0 ($= 293$ K), R the constant of perfect gases, Q the activation energy of the diffusion process ($Q/R \approx 4,700$ K).

Hence, equation (3a) can be re-written as:

$$\mathbf{J} = -\mathrm{agradh}. \tag{6a}$$

The Soret flux (thermal moisture flux) is already incuded in equation (6a); this is because:

$$\mathrm{gradh} = \mathrm{grad}\frac{p_{gw}}{p_{gws}} = \frac{1}{p_{gws}}\left[\left(\frac{\partial w}{\partial p_{gw}}\right)\mathrm{grad}p_{gw} + \left(\frac{\partial w}{\partial T}\right)\mathrm{grad}T\right], \tag{6b}$$

which follows by differentiating the sorption relation $w = w(p, T)$.

The continuity equation for non-isothermal flow is finally obtained as (Schrefler *et al.*, 1989; Majorana *et al.*, 1997, 1998; Salomoni *et al.*, 2007):

$$\frac{\partial h}{\partial t} - \nabla^T\mathbf{C}\nabla h - \frac{\partial h_s}{\partial t} - k\frac{\partial T}{\partial t} + \chi\mathbf{m}^T\frac{\partial \boldsymbol{\varepsilon}}{\partial t} = 0, \tag{7}$$

where $\mathbf{C}$ is the (relative humidity) diffusivity diagonal matrix.

The heat balance requires that:

$$\rho C_q\frac{\partial T}{\partial t} - C_a\frac{\partial w}{\partial t} - C_w\mathbf{J}\cdot\nabla T = -\mathrm{div}\mathbf{q}, \tag{8}$$

where ρ is the mass density of concrete, C_q the isobaric heat capacity of concrete (per kilogram of concrete) including chemically bound water but excluding free water, C_a the heat of absorption of free water (per kilogram of free water); C_w is the isobaric heat capacity of bulk (liquid) water; $C_w\mathbf{J}\cdot\nabla T$ is the rate of heat supply due to convection by moving water and $\mathbf{q}$ is the heat flux. Usually, the term of heat convection is negligible, but in rapid heating it might not be so. The heat of vaporization of water

does not figure explicitly, but it may be included within the second term of the left hand side expression (Bažant and Thonguthai, 1979).

The heat flux **q** is due to temperature gradient (governed by Fourier's law) and to moisture concentration gradient (Dufour's flux):

$$\mathbf{q} = -a_{Tw}\nabla w - a_{TT}\nabla T, \tag{9a}$$

where the coefficients a_{Tw}, a_{TT} depend on w and T.

Owing to the negligible contribution of the moisture flux, equation (9a) is re-written as:

$$\mathbf{q} = -a_{TT}\nabla T, \tag{9b}$$

and a_{TT} is the heat conductivity.

Equation of state for pore water

For temperatures $T < 647.3\,K$ (critical point of water) we must distinguish between saturated and partially saturated concrete. A saturated state for concrete can be referred to the value of h or to another variable, the degree of saturation, linked to h through a pressure called capillary pressure (Gawin *et al.*, 1999; Grasley and Lange, 2007):

$$p_c = -\frac{\rho_w RT}{M_w}\ln h, \tag{10}$$

in which $\rho_w = \rho_w(p, T)$ is the liquid water density (see below) and M_w is the molecular weight of water.

The degree of saturation is calculated, starting from Baroghel-Bouny *et al.* (1999), as:

$$S = \begin{cases} \left[\dfrac{\left(\frac{T_{cr}-T_0}{T_{cr}-T}\right)^N}{a^*}p_c\right]^{b/(b-1)} & T \le T_{cr} \\ \frac{N}{z^{N+1}}(T_{cr}-T_0)^N T + \left(\frac{T_{cr}-T_0}{z}\right)^N\left[1-\frac{N}{z}(T_{cr}-z)\right] & T > T_{cr} \end{cases}, \tag{11}$$

in which T_{cr} is the critical temperature of water, N an empirical parameter ($= 1.2$), z a parameter governing the transition through the critical temperature of water ($= 0.5\,K$), b a constant ($= 2.2748$). Parameter a^* is a function of temperature:

$$a^* = \begin{cases} Q_3 = 18.6237\ \text{MPa} & T \le 373.15\ K \\ \text{with } Q_2 = 7\ \text{MPa}, Q_0 = (Q_3 - Q_2)\left[2\left(\frac{T-373.15}{T_{cr}-373.15}\right)^3 - 3\left(\frac{T-373.15}{T_{cr}-373.15}\right)^2 + 1\right] + Q_0 + Q_2 & T > 373.15\ K \end{cases} \tag{12}$$

The expression in equation (11) is a proposal for upgrading the Baroghel-Bouny's desorption isotherms to account for high-temperature effects (Khoury and Majorana, 2007).

Using such an approach it is possible to skip a problem arising when using Bažant's model, i.e. under the critical point of water the water content is considered as liquid water (free water plus a small percentage for bound water), while when T overcomes the critical point, the residual water has to be considered as gas water or a monolayer of physically bound water. Differently, through this upgraded approach, it is possible to have a consistent amount of water also above critical temperature, representing the gas phase and the chemically bound water in this zone which are separately computed.

Partially saturated concrete. From experimental data (England and Ross, 1970; Zhukov and Shevchenko, 1974) it was seen that the following semi-empirical expression is acceptable:

$$\frac{w}{c} = \left(\frac{w_1}{c}\, h\right)^{1/m(t)} \quad \text{for } h \le 0.96, \tag{13}$$

in which:

$$m(t) = 1.04 - \frac{t'}{22.34 + t'}, \quad t' = \left(\frac{t+10}{t_0+10}\right)^2, \tag{14}$$

with t expressed in °C; $t_0 = 25$°C; c is the (dried) cement mass per m^3 of concrete; w_1 is the saturation water content at 25°C.

Saturated concrete. In saturated states (Figure 7), the thermodynamic properties of water can be taken into account in terms of specific volume of water, υ, as a function of T and p, $\upsilon = \upsilon(T, p)$. In this way, the effect of porosity variation and of volumetric elastic expansion can be described by Powers and Brownyard (1947):

$$w = \frac{(1 + 3\varepsilon^v)n}{\upsilon} \quad \text{for } h = 1, \tag{15}$$

where:

$$d\varepsilon^v = \frac{d\sigma^v}{3\bar{K}} + \alpha dt, \quad \sigma^v = np, \tag{16}$$

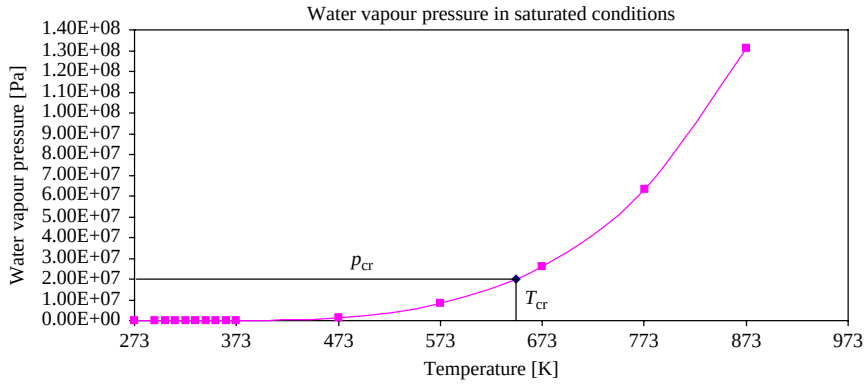

Notes: S = 1; pc = 0

Figure 7.
Water vapor pressure under h = 1

with n porosity, ϵ^{v} volumetric strain of concrete due to the stress σ^{v}, $\bar{K}$ volumetric modulus, α coefficient of linear thermal expansion of concrete (typically, 12×10^{-6}°C^{-1}), and p pore water pressure (Bažant *et al.*, 1988), i.e. an average pressure of the mixture of fluids filling the voids, which takes the form:

$$p = p_g - p_c - p_{atm}, \tag{17}$$

where p_g is the moist air pressure (defined below) and p_{atm} the atmosperic pressure.

A more interesting approach is presented in Grasley and Lange (2007), following the approach of Bentz *et al.* (1998), according to which the linear strain associated with the pressure change within the pore fluid can be expressed as:

$$\varepsilon = \Delta p S \left[\frac{1}{3k_s} - \frac{1}{k_{ss}}\right], \tag{18}$$

in which Δp is calculated by subtracting p_c calculated from equation (10) prior to the temperature change from the p_c calculated from equation (10) after the temperature change, k_s is the bulk modulus of the porous solid, k_{ss} the bulk modulus of the solid skeleton of the material and S (there defined as saturation factor) is referable to the degree of saturation of equation (11).

Concrete permeability. It is assumed that the flux of moisture inside the concrete is controlled by the minimum transverse section of the pores, or "necks", in the flux tubes through the cement paste.

An acceptable form for permeability (Bažant and Najjar, 1972) is:

$$\text{for } t \leq 95°C, \quad a = a_0 f_1(h) \cdot f_2(t) \tag{19a}$$

$$\text{for } t > 95°C, \quad a = a_0' f_3(t) \tag{19b}$$

with $a_0' = a_0 f_2(95°C)$; a_0 is the reference permeability at 25°C.

The temperature of 95°C is chosen as the beginning of this transition. The function $f_1(h)$ reflects the moisture transfer in the layers of water adsorbed inside the necks and in agreement with (Bažant and Najjar, 1972; Bažant, 1975a):

$$\begin{gathered} f_1(h) = \bar{\alpha} + \frac{1-\bar{\alpha}}{1+((1-h)/(1-h_c))} \quad \text{for } h < 1 \\ f_1(h) = 1 \quad \text{for } h = 1 \end{gathered}, \tag{20}$$

where $h_c \cong 0.75 = \text{humidity of transition}$, $\bar{\alpha} \cong 1/20$ at 25°C.

At $t = 95$°C, it is assumed that the necks are sufficiently large to allow the flow of both liquid water and water vapour phases. Hence, $\bar{\alpha}$ is equal to 1 at 95°C. Between 25 and 95°C a linear interpolation of $\bar{\alpha}$ is assumed. If the curve is extended below 25°C, the relation $1/\bar{\alpha} = 1 + 19(95 - t)/70$ seems more appropriate.

f_2 in equation (19a) is given by an Arrhenius' type equation:

$$f_2(T) = e^{[(Q'/R)((1/T_0)-(1/T))]} \quad T < 368.15 \text{ K}(95°C), \tag{21}$$

with Q' activation energy for the migration along the multimolecolar layers of water adsorbed inside the necks.

In accordance with Bažant and Najjar (1972) $Q'/R \cong 2,700$ K, and a good choice for $f_3(T)$ is given by:

$$f_3(T) = e^{[(t-95)/(0.881+0.214(t-95))]} \quad t > 95°C. \tag{22}$$

The permeability is also largely influenced by the hydration degree (or aging). Referring to the available data, this dependence seems to be well described by:

$$a_0 = a_1 \cdot 10^{\sqrt{a_2/t_e}}. \tag{23}$$

The values of $a_1 = 10^{-13}$ m/s, $a_2 = 40$ days agree with the data by Powers and Brownyard (1947).

The effect of thermo-mechanical damage on permeability (not reported here) is being implemented.

Hydration and drying of concrete. The hydration degree can be conveniently referred to the period of equivalent hydration, t_e, which represents the period of hydration at 25°C in water, necessary to confer the same hydration degree which is assumed at the real time t and with the actual history of variable h and t. It is defined, for $0 < t < 100$°C, as:

$$t_e = \int_0^t \beta_T \beta_h dt. \tag{24}$$

The coefficient β_T is a function of temperature and, since the chemical reaction of hydration is a process which is thermally activated, it can be expressed as (Bažant, 1975a):

$$\beta_T = e^{[(Q_h/R)((1/T_0)-(1/T))}, \quad \beta_h = [1 + \alpha^*(1 + h)^4]^{-1}, \tag{25}$$

where Q_h is the activation energy of hydration (Bažant and Najjar, 1972) and α^* varies between 5 and 7.5 (Bažant and Najjar, 1972; Bažant and Panula, 1979; Bažant and Wittmann, 1982; Bažant, 1986).

From the interpolation of experimental results by Powers and Brownyard (1947) at 25°C, the hydrated water takes the form:

$$w_h(t_e) \approx 0.21c\left(\frac{t_e}{\tau_e + t_e}\right)^{1/3} \quad \tau_e = 23 \text{ days}. \tag{26}$$

The total amount of free water (evaporable) w_d (per m^3 of concrete), can be expressed as:

$$w_d = w_h^{105} f_d(T), \tag{27}$$

where w_h^{105} represents the hydrated water content at 105°C and typical values for $f_d(T)$ are reported in Harmathy and Allen (1973).

Additional constitutive and thermodynamic relationships for the description of hygro-thermal states of concrete

The liquid water density of equation (10) can be calculated through a linear relationship of both temperature and water pressure p_w ($p_w = p_g - p_c$) (Reid *et al.*, 1987; Bear, 1988; Forsyth and Simpson, 1991):

$$\rho_w = \rho_{w0}[1 - \beta_w(T - T_0) + \alpha_w(p_w - p_{atm})](\text{if } T \geq T_{cr}, \text{ then } T = T_{cr}), \quad (28)$$

in which ρ_{w0} is the liquid water density at reference temperature T_0 and pressure p_{atm} ($= 999.84\,kg/m^3$), β_w the volumetric thermal expansion coefficient of water (see below) and α_w the isothermal compression modulus of water.

The state equation of liquid water is valid for bulk free liquid water, but it is also often used for the description of capillary and bound water. However, due to the complex nature of the interaction between the water and the solid skeleton, its applicability is questionable, especially as far as pressure dependence is concerned (although capillary water is in traction, but its density is not expected to be lower than that for bulk water). Sometimes (and ours is the case) this relationship is used assuming water incompressibility, i.e. $\alpha_w = 0$, taking into account that, close to the critical point of water, a sharp increase in β_w takes place.

Typical values of β_w are $0.68 \times 10^{-4}\,K^{-1}$ if $T = 273.15\,K$, and $10.1 \times 10^{-4}\,K^{-1}$ if $T = 420\,K$; its relationship with temperature is non-linear, hence the present authors propose the following expression:

$$\beta_w(T) = 4 \times 10^{-7} e^{0.0184T}. \quad (29)$$

For water vapour and moist air, the Clapeyron equation of state (EOS) of perfect gases:

$$p_{gw} = \frac{\rho_{gw} RT}{M_w}, \quad p_g = \frac{\rho_g RT}{M_g}, \quad (30)$$

and Dalton's law:

$$p_g = p_{ga} + p_{gw}, \quad (31)$$

are assumed as state equations. The dry air pressure p_{ga} in our approach has been evaluated using iteratively the virial EOS (Hyland and Wexler, 1983; Wylie and Fisher, 1996; Jayaraman, 1999; Ji *et al.*, 2003; Ji and Yan, 2006), to adjust the non-ideal behaviour of the vapour phase (the same approach could be followed for both vapour and moist air), with indications by ASHRAE (1989) for calculating dry air density. The virial EOS takes the form:

$$\frac{p_{ga} v'}{RT} = 1 + \frac{B_{aa}}{v'} + \frac{C_{aaa}}{v'^2}, \quad (32)$$

where v' is the molar volume of dry air and B_{aa}, C_{aaa} are the second and third virial coefficient, respectively, given by:

$$B_{aa}[cm^3/mol] = \sum_{i=0}^{3} B_i T^{-i} \quad C_{aa}[cm^6/mol^2] = \sum_{i=0}^{3} C_i T^{-i}, \quad (33)$$

with B_i and C_i listed in Table II.

As regards moisture transport, being the moisture flow still governed by a differential equation expressed in terms of pores' relative humidity (equation (7)), the authors propose to express the equation deriving the velocity of water flow, in accordance with Shazali *et al.* (2006), as:

$$\mathbf{v}_h = -C(h)\nabla h, \tag{34}$$

in which the correlation between the relative humidity and material water content is already guaranteed by using adsorption and desorption isotherms.

However, regarding both capillary water and gas phase, significant deviations from the multiphase Darcy's law have been observed in tests involving gas flow though concrete (Klinkenberg, 1941; McVay and Rish, 1995; Li and Horne, 2001): pressure driven transport conditions involving gases flowing through cementitious materials do not generally obey Darcy's law for laminar fluid flow. The rate of mass flow through the material exceeds that predicted either microscopically within the flow channels from Poiseuille's law or macroscopically from Darcy's law.

Hence, the effect of gas slip flow is here calculated, by neglecting the effect of gravitational acceleration, according to (Chung *et al.*, 2006):

$$\eta_g \mathbf{v}_g = -\frac{a'_g}{\mu_g}\left(1+\frac{b}{p_g}\right)\nabla p_g, \tag{35a}$$

where η_g is the gas phase volume fraction, a'_g the intrinsic permeability to gas, μ_g the gas-phase dynamic viscosity, b is called the slip flow constant (or Klinkenberg constant) and the term within parenthesis is the slip-modification factor. A relationship between a'_g and b is proposed by Chung and Consolazio (2005):

$$b = e^{(-0.5818\ln(a'_g)-19.1213)}. \tag{35b}$$

Finite element discretization

The application, within the numerical code DAMVIS, of a standard finite element discretization in space of equations (7) and (8) (the linear momentum equation is included for completeness, but its expression has not reported previously for sake of brevity) results in:

$$\begin{bmatrix} \mathbf{K} & \mathbf{HU} & \mathbf{TU} \\ \mathbf{L}^T & \mathbf{I} & \mathbf{TP} \\ 0 & \mathbf{TH} & \mathbf{TS} \end{bmatrix} \begin{Bmatrix} \dot{\bar{\mathbf{u}}} \\ \dot{\bar{\mathbf{h}}} \\ \dot{\bar{\mathbf{T}}} \end{Bmatrix} + \begin{bmatrix} 0 & 0 & 0 \\ 0 & \mathbf{Q} & 0 \\ 0 & 0 & \mathbf{TR} \end{bmatrix} \begin{Bmatrix} \bar{\mathbf{u}} \\ \bar{\mathbf{h}} \\ \bar{\mathbf{T}} \end{Bmatrix} = \begin{Bmatrix} \dot{\mathbf{f}} + \mathbf{c} \\ \dot{\mathbf{HG}} \\ \dot{\mathbf{TG}} \end{Bmatrix}, \tag{36}$$

in which $\bar{\mathbf{u}}$, $\bar{\mathbf{h}}$ and $\bar{\mathbf{T}}$ are the nodal values of the basic variables and the matrices take the form:

i	B	C
0	0.349568×10^2	0.125975×10^4
1	-0.668772×10^4	-0.190905×10^6
2	-0.210141×10^7	0.632467×10^8
3	0.924746×10^8	–

Table II. Parameters B_i and C_i for calculating the coefficients in the virial EOS for dry air

$$
\begin{aligned}
\mathbf{K} &= -\int_{\Omega} \mathbf{B}^{\mathrm{T}}\mathbf{D}_{\mathrm{T}}\mathbf{B}\mathrm{d}\Omega \\
\mathbf{HU} &= \int_{\Omega} \mathbf{B}^{\mathrm{T}}\mathbf{D}_{\mathrm{T}}\boldsymbol{\kappa}\mathbf{N}\mathrm{d}\Omega \\
\mathbf{TU} &= \int_{\Omega} \mathbf{B}^{\mathrm{T}}\mathbf{D}_{\mathrm{T}}\boldsymbol{\alpha}\mathbf{N}\mathrm{d}\Omega \\
\mathbf{L}^{\mathrm{T}} &= \int_{\Omega} \mathbf{N}^{\mathrm{T}}\mathbf{m}^{\mathrm{T}}\chi\mathbf{B}\mathrm{d}\Omega \\
\mathbf{TP} &= -\int_{\Omega} \mathbf{N}^{\mathrm{T}}\mathrm{k}\mathbf{N}\mathrm{d}\Omega \\
\mathbf{Q} &= \int_{\Omega} (\nabla\mathbf{N})^{\mathrm{T}}\mathbf{C}(\nabla\mathbf{N})\mathrm{d}\Omega \\
\mathbf{TH} &= \int_{\Omega} \mathbf{N}^{\mathrm{T}}\left((1-\phi)\mathrm{C_s}\frac{\rho_{\mathrm{s}}}{\mathrm{k_s}} + \phi\mathrm{C_{moist}}\frac{\rho_{\mathrm{moist}}}{\mathrm{k_{moist}}}\right)\mathbf{N}\bar{\mathbf{T}}\mathbf{N}\mathrm{p_{gws}}\mathrm{d}\Omega \\
\mathbf{TS} &= \int_{\Omega} \mathbf{N}^{\mathrm{T}}\rho\mathrm{C_q}\mathbf{N}\mathrm{d}\Omega \\
\mathbf{TR} &= \int_{\Omega} (\nabla\mathbf{N})^{\mathrm{T}}\Lambda(\nabla\mathbf{N})\mathrm{d}\Omega - \int_{\Omega} (\nabla\mathbf{N})^{\mathrm{T}}\rho_{\mathrm{moist}}\mathrm{C_{moist}}\mathbf{V}_{\mathrm{h}}\mathbf{N}\mathrm{d}\Omega \\
\mathbf{c} &= -\int_{\Omega} \mathbf{B}^{\mathrm{T}}\mathbf{D}_{\mathrm{T}}\mathbf{D}_{\mathrm{T}}^{-1}\sum_{\mu=1}^{\mathrm{N}}\frac{\varphi_{\mathrm{T}}\varphi_{\mathrm{h}}}{\tau_{\mu}}\boldsymbol{\sigma}_{\mu}\mathrm{d}\Omega \\
\mathrm{d}\mathbf{f} &= -\int_{\Omega} \mathbf{N}^{\mathrm{T}}\mathrm{d}\mathbf{b}\mathrm{d}\Omega - \int_{\Gamma} \mathbf{N}^{\mathrm{T}}\mathrm{d}\hat{\mathbf{t}}\mathrm{d}\Gamma - \int_{\Omega} \mathbf{B}^{\mathrm{T}}\mathbf{D}_{\mathrm{T}}\mathrm{d}\varepsilon_0\mathrm{d}\Omega \\
\mathbf{HG} &= \int_{\Omega} \mathbf{N}^{\mathrm{T}}\mathrm{h_s}\mathrm{d}\Omega \\
\mathbf{TG} &= -\int_{\Omega} \mathbf{N}^{\mathrm{T}}\mathrm{Q_h}\mathbf{N}\mathrm{d}\Omega - \int_{\Gamma} \mathbf{N}^{\mathrm{T}}\mathrm{q_h}\mathrm{d}\Gamma
\end{aligned}
\qquad (37)
$$

where **HU** and **TU** account for shrinkage and thermal dilation effects, respectively; $\mathbf{L}^{\mathrm{T}}$ and **TP** are the coupling matrices representing the influence of the mechanical and thermal field on the hygral one, respectively; **Q** is the diffusivity matrix accounting for sorption-desorption isotherms; **TH** the coupling matrix between the hygral and thermal fields in terms of capacity; **TS** the matrix of heat capacity; **TR** the matrix of thermal transmission including the convective term; **c** the matrix accounting for creep; **HG** the matrix of humidity variation due to drying and **TG** accounts for heat fluxes.

For further explanations of the above terms the reader is referred to Schrefler *et al.* (1989), Majorana *et al.* (1998) and Majorana and Salomoni (2004).

Predictor-corrector iterative scheme

The proposed iterative scheme solves the upgraded non-linear convection-diffusion model between a predictor and a corrector phase (Goldschmit and Cavaliere, 1997; Cheng *et al.*, 2003), taking into account the addition of thermodynamic relations. The heat of vaporization is included.

The scheme allows for restoring the full coupling of the mathematical model in which the basic equations (see the previous section) are expressed in weak form, supplemented by additional equations in their strong form: hence capillary pressure and gas pressure are obtained as secondary variables, but the correctness of their values (and, correspondingly, the non-linear geometric feature of the model as a whole) is proposed to be recovered just through a PC iterative scheme.

The following numerical strategy is implemented and first details are reported below:

Starting procedure:

- $i = 0$ (i iteration counter); and
- initial guess for $\mathbf{u}^0$ (displacement vector, see next section), h^0, T^0 (e.g. obtained from a zero equation model solution).

Predictor phase:

- (P1) $i = i + 1$.
- (P2) Solve moisture and heat balance equations (7) and (8) neglecting the coupling term with the mechanical field.
- (P3) Solve equation (32) using the Newton-Raphson iteration method and determine p_{ga}.
- (P4) Calculate (p_{gw}, p_c, S), p_g (equations (2), (10), (11), (31)).
- (P5) Solve the linear momentum equation (Majorana *et al.*, 1998) for $\mathbf{u}$.
- (P6) Repeat from (P2) until convergence is achieved, both in a h-norm and in a T-norm ($h^{(i)}$ and $T^{(i)}$ are the converged values).

Corrector phase:

- (C1) Determine h from equation (10).
- (C2) Solve iteratively moisture and heat balance equations for $\mathbf{u}$ and T (coupling term included) until convergence is achieved in a $\mathbf{u}$-norm ($\mathbf{u}^{(i)}$ is the converged value).
- (C3) Update p_{ga} from equation (32).

Convergence check. Repeat the predictor and corrector phase until convergence is achieved, in a h-, T-, $\mathbf{u}$-norm.

The convergence criteria adopted are:

- predictor phase: $\text{Norm}(h) \leq h\text{TOL}$ and $\text{Norm}(T) \leq \text{TTOL}$;
- corrector phase: $\text{Norm}(\mathbf{u}) \leq \mathbf{u}\text{TOL}$;
- complete corrector/predictor algorithm: $\text{Norm}(h) \leq h\text{TOL}$, $\text{Norm}(T) \leq \text{TTOL}$, $\text{Norm}(\mathbf{u}) \leq \mathbf{u}\text{TOL}$, with:

$$\text{Norm}(x) = \frac{\|x^s - x^{s-1}\|_{L_2}}{\|x^s\|_{L_2}},$$

and TOL convergence tolerance.

To give some additional details about the proposed PC scheme, let us consider the system of equations (36) neglecting the coupling with the mechanical field (Step (P2)), re-written in a compact form as:

$$\mathbf{B}\dot{\mathbf{X}} + \mathbf{C}\mathbf{X} = \mathbf{F}, \quad \mathbf{X} = \{h, T\}^T. \tag{38}$$

Discretizing in time equation (38), e.g. following Turska and Schrefler (1993), we obtain:

$$[\mathbf{B} + \theta\Delta t\mathbf{C}]\mathbf{X}_{n+1} = [\mathbf{B} - (1 - \theta)\Delta t\mathbf{C}]\mathbf{X}_n + \Delta t\mathbf{F}_{n+\theta}, \tag{39}$$

where Δt is the time step length, $\mathbf{X}_{n+1}$ and $\mathbf{X}_n$ are the state vectors at time instant t_{n+1} and t_n, and θ is a parameter (usually $0 \leq \theta \leq 1$) of the "generalized midpoint rule" used.

Equation (39) can be solved, e.g. by a staggered procedure performed after partitioning the matrix$\mathbf{D} = \mathbf{B} + \theta\Delta t\mathbf{C}$; the predictor $\mathbf{X}_{n+1} = \mathbf{X}_{n+1}^{(P)}$ is obtained after rearranging equation (39). Usually, $\mathbf{X}_{n+1}^{(P)}$ depends linearly on the already calculated values $\mathbf{X}_{n-i}$.

Hence, the displacement vector in system (36) can be directly calculated after steps (P4-P5), e.g. in accordance with what proposed in Salomoni and Schrefler (2005), and finally $\bar{\mathbf{X}}_{n+1}^{(P)} = \{\mathbf{u}, h, T\}^T$ is obtained.

Once the predictor is set and convergence achieved (P6), it is then corrected after direct evaluation of h_n, h_{n+1} (C1); (C2) leads to obtain a system similar to equation (38), where now $\mathbf{X} = \{\mathbf{u}, T\}^T$ and the corrector is finally reached, i.e. $\bar{\mathbf{X}}_{n+1}^{(C)} = \{\mathbf{u}, h, T\}^T$.

The final convergence check allows for checking:

$$\frac{\left|\mathbf{X}_{n+1}^{(C)} - \mathbf{X}_{n+1}^{(P)}\right|_{L_2}}{\left|\mathbf{X}_{n+1}^{(C)}\right|_{L_2}} \leq \mathrm{TOL},$$

with TOL a suitable convergence tolerance.

Numerical analyses

A conical tank for storing hot salts has been modelled through the FE research code DAMVIS (Figure 8) using 330 eight-node isoparametric elements (axis-symmetric condition). In agreement with the design criteria, it is proposed to employ a HPC, particularly C90 for this analysis, to increase both the operational temperature up to 120°C – against the usual 90°C for ordinary concretes – and concrete durability. The whole tank is composed by a flat stainless steel liner in contact with the salts and a

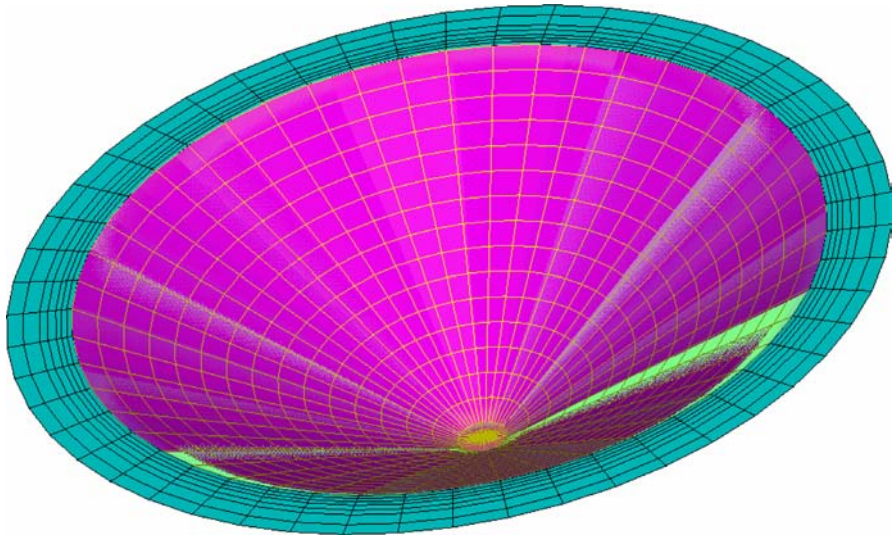

Figure 8.
FE discretization for the thermal storage concrete tank

ceramic fibre blanket (not modelled here) close to the concrete main structure (Figure 5). An additional passive cooling system is supposed to be added within the concrete thickness to reach such operational temperature on concrete surfaces. Geometric details have not been included for privacy reasons.

The adopted material properties are listed in Table III.

The concrete tank is subjected to transient heating from the internal side assuming to reach the maximum temperature of 100°C in eight days; the concrete tank has initially a relative humidity of 60 per cent and a temperature of 30°C. In the first analyses (pushed up to about four months) the tank is supposed to be simply supported on its basement only. For sake of clarity, structural constraints, initials and boundary conditions adopted in the two main numerical analyses are shown in Figure 9.

The results in terms of RH are shown in Figure 10 (3D plot): the development of the RH bowl in time (along section B-B, see Figure 11) is clearly evident; the peaks in RH for the zone closest to the heated surface (see the contour map of Figure 13(a)) are not

Water/cement ratio	0.29
Elastic modulus (MPa)	0.367×10^{5}
Poisson's ratio	0.18
Reference diffusivity along x/y directions (mm^2/day)	0.1×10^{2}
Intrinsic liquid permeability (mm^2)	2.0×10^{-19}
Unrestrained shrinkage for h = 0 (ϵ_{sh})	-0.4×10^{-2}
Thermal expansion coefficient of solid	0.12×10^{-4}
Hygro-thermal coefficient	0.5×10^{-2}
Thermal capacity (N/(mm^2 K))	2.0
Heat conductivity along x/y directions (N/(day K))	0.18144×10^{6}
Coefficient α_0 for diffusivity	0.5×10^{-1}

Table III.
Material parameters for concrete C90

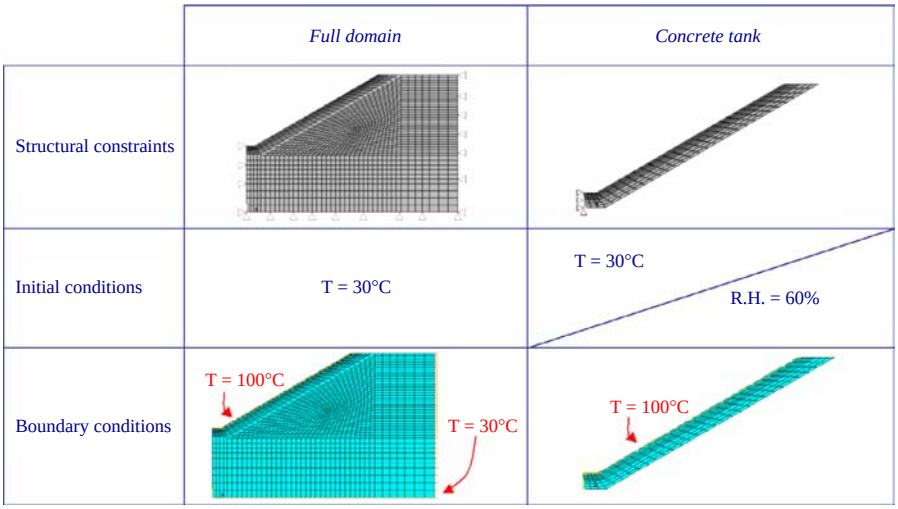

Figure 9.
Structural constraints, initials and boundary conditions for the numerical analyses

referable to the phenomenon of "moisture-clog" (Majorana *et al.*, 1998; Chung *et al.*, 2006), because of the limited value of the temperature gradient (Figures 12 and 13(b)), but anyway it is driven by the coupling between humidity and temperature fields and it is connected to the low-intrinsic liquid permeability of the adopted HPC. Once 100°C has been reached, concrete starts depleting itself of water, thereby making the relative humidity values tend towards zero (but very slowly: in fact, after about four months, a concrete thickness of about 255 mm is still in saturated conditions).

Correspondingly, for the same section, the thermal wave is depicted in the 3D plot of Figure 12: after one month all the thickness is heated at about 100°C; consequently, it has been verified (the details cannot be reported here) that the reached mean damage level by the concrete structure is lower than 50 per cent.

The peaks in water vapour pressure (Figure 14) slowly increase up to about 0.1 MPa after 16.8 days (the results refer to section A-A), with the peak moving slowly towards the external part of the tank; at later times the phenomenon is reversed, with a decrease in vapour pressure close to the heated surface and a trend to reach a uniform value on the opposite side.

The results of saturation at time stations t = 1.6, 12, 16.8, 24, 48 and 110 days are additionally shown in Figure 15: an increase of desaturation occurs only after 16.8 days (peak of RH) in a zone which enlarges as time proceeds. The desaturation is mainly caused by the evaporation of water inside the tank, resulting in formation of a zone of

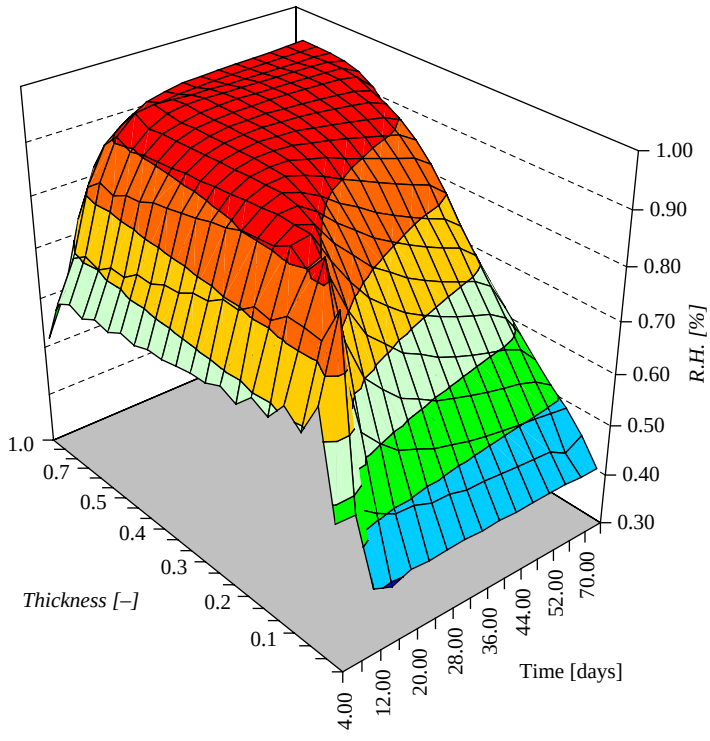

Figure 10.
RH time-history along section B-B

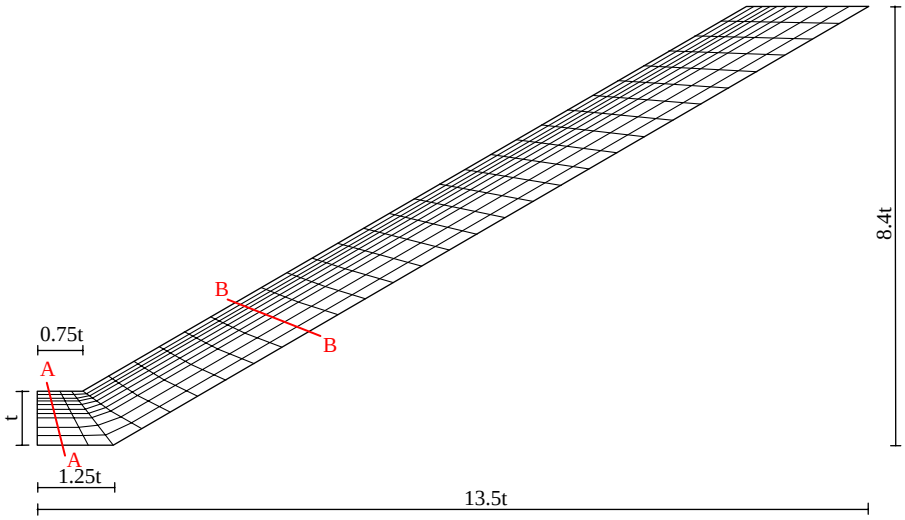

Figure 11.
Locations of sections A-A and B-B

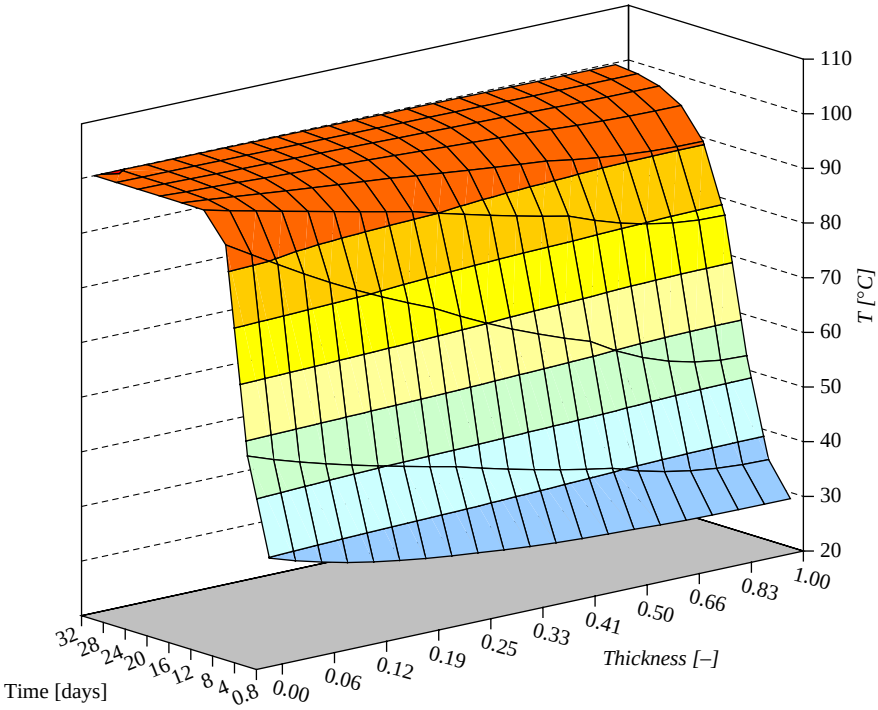

Figure 12.
Thermal wave along section B-B

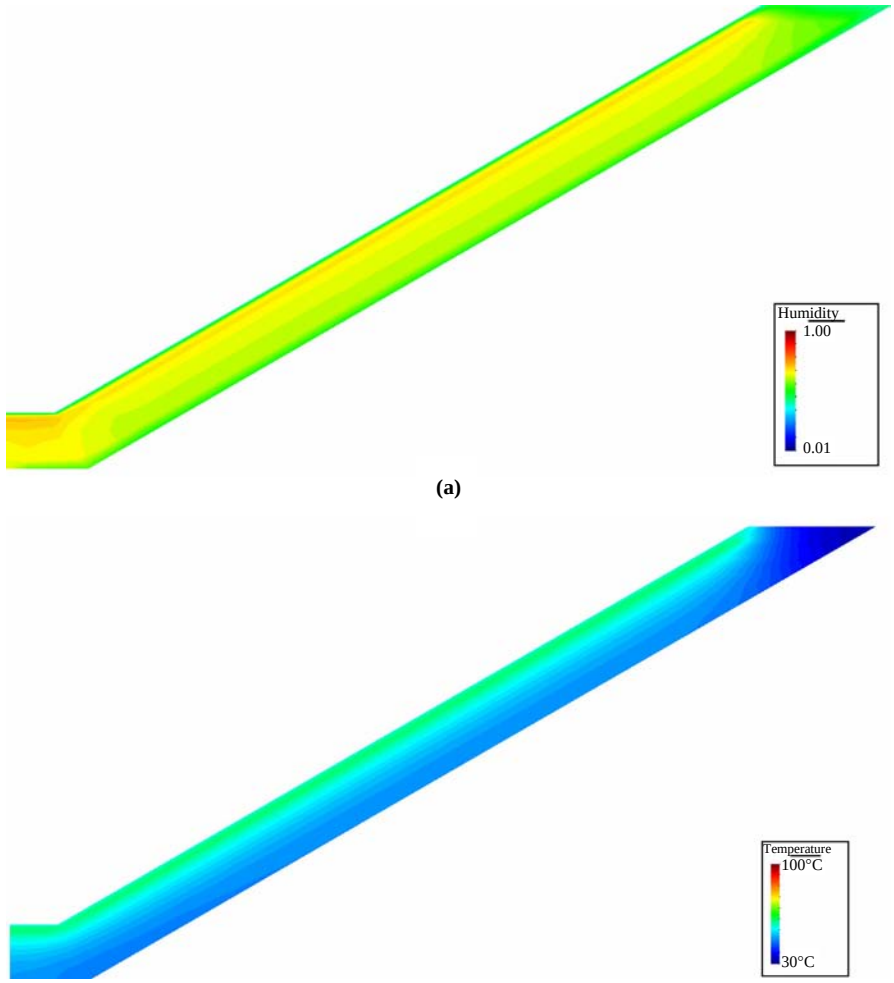

Figure 13.
Contour maps of RH (a) and T (b) at time station t = 8.8 day

increased vapour pressure (see Figure 14 for section A-A; the trend is maintained for section B-B). Vapour pressure gradients cause vapour flow towards both the heated surface and the external side of the tank. Moreover, the existing temperature gradient causes thermo-diffusion of water vapour towards the colder layer of the wall. These vapour flows result in an increase in RH above its initial value (Figure 10) as well as in condensation of vapour in the colder layers and subsequent slight increase in saturation.

The effect of a surrounding ground volume (dry sand) has been additionally evaluated (Figure 16) on the development of the thermal front up to five months; it has been assumed to fix the temperature along the domain boundaries (both vertical and horizontal ones located at a distance of 5t from the tank's edges) at 30°C to check if the

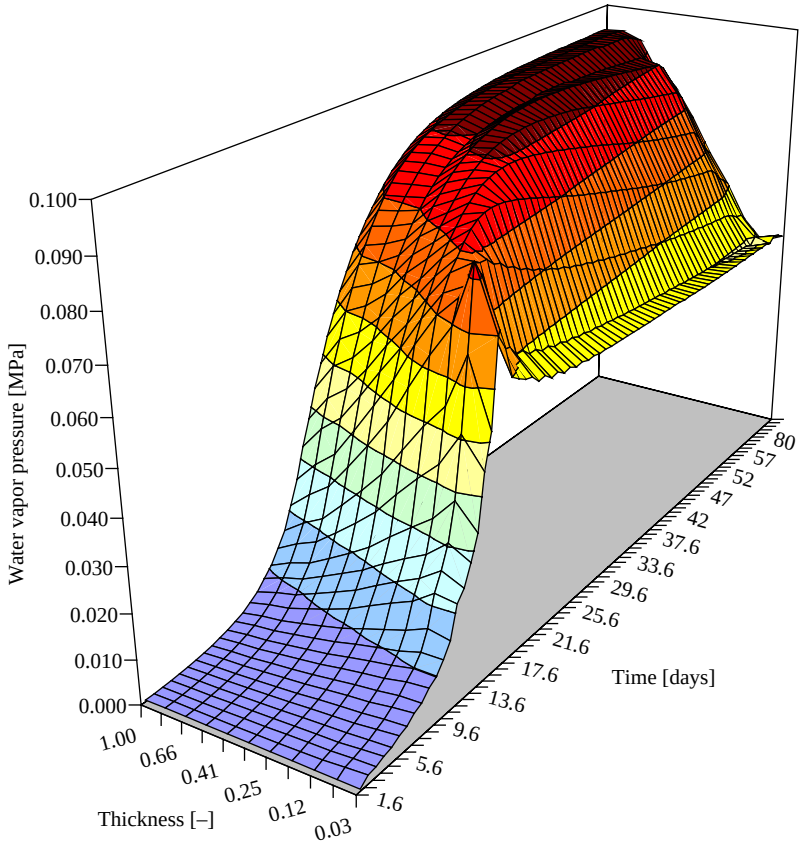

Figure 14.
Water vapor pressure along section A-A

thermal isolines have reached equilibrium at the end of the analysis or if this has to be pushed up further. At present, considering larger domains is not supported by design evidences. Interfacial (tank-ground) elements have been added to allow for relative displacements.

The sand is supposed to be characterized by a specific heat of 781.25 J/(kg K) and a thermal conductivity of 0.35 W/(m K); the time-history of temperature for the external node belonging to section B-B (interface between concrete and ground) is shown in Figure 17, comparing the results obtained by the analysis for the tank only: the difference in the curves slope is partly due to the adopted way for applying the thermal load (now no more ramped; anyway the effect is extinguished within the first 10-20 days) and mainly to the thermal inertia of the ground, which leads to shift the maximum temperature to farther times. Additionally, the peak of 100°C seems to be not reachable even after several months.

The situation is clearly preferable when considering the durability performances of the concrete tank, but anyway the heat level is again not admissible for the soil: under such temperatures chemical reactions can take place if organic materials are present, even if a soil treatment is usually performed; moreover, a desiccation of zones around

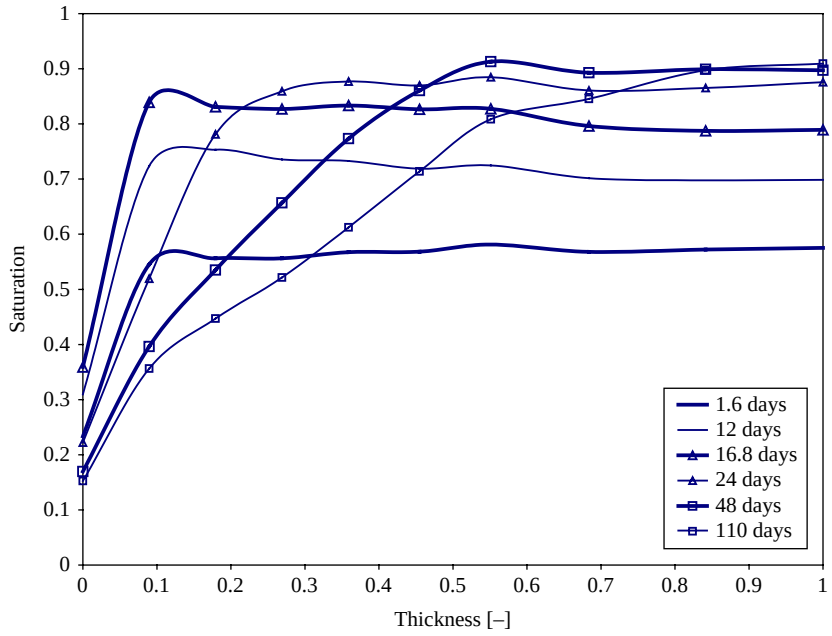

Figure 15.
Saturation along section B-B

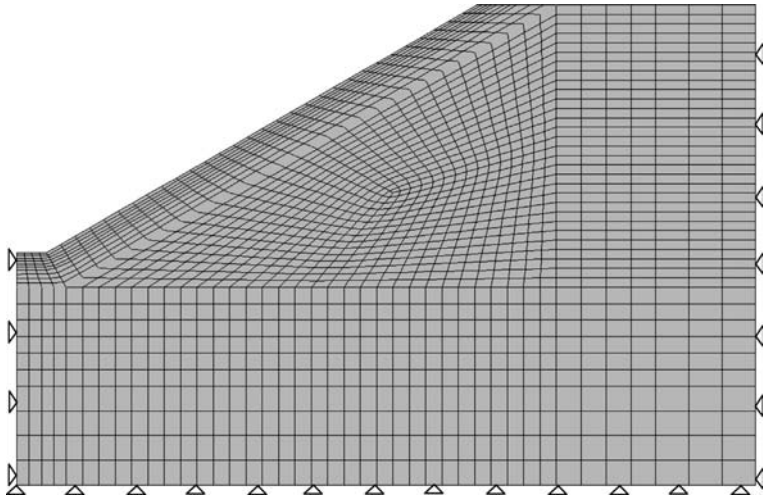

Figure 16.
Adopted discretization for the whole domain (tank + ground)

the tank combined with possible re-wettings due to rainfalls could induce relative displacements and consequently tank movements. Hence, being the hypothesis of an additional cooling system (or an additional foundation) too expensive in the design of such structures, it should be planned to use gravelly soils when preparing the surrounding embankment.

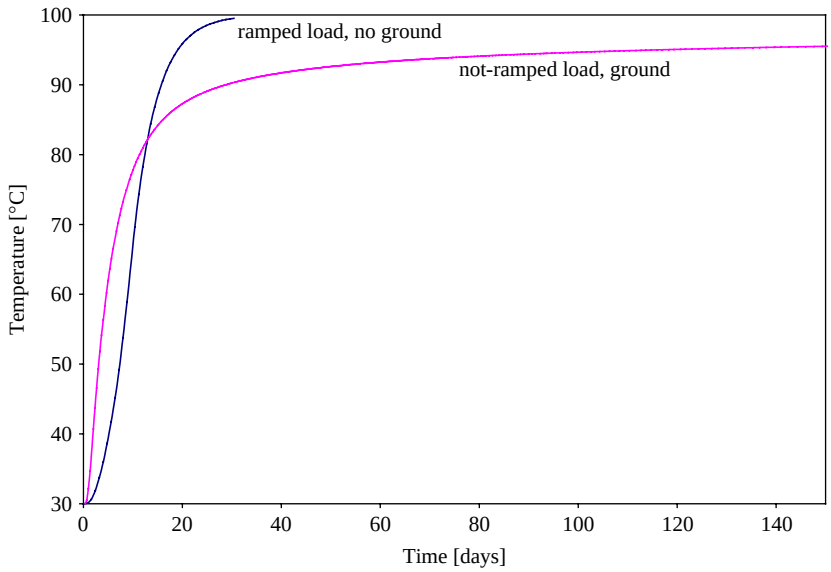

Figure 17.
Time-history of temperature (tank alone and whole domain)

The contour plots of temperature after five months are shown in Figures 18 and 19 (section): the isolines do not seem to have reached equilibrium yet, so that the analysis has been pushed up to about two years to catch thermal equilibrium within the investigated volume (Figure 20).

Conclusions

An experience of R&D in the field of new technologies for solar energy exploitation within the Italian context has been described. Within the medium temperature field, an innovative approach has been presented for the conceptual design of liquid salts concrete storage systems. A multi-tank sensible-heat storage system has been proposed for storing thermal energy, with a two-tanks molten salt system. The hygro-thermal behaviour of a HPC tank has been assessed through a coupled FE code based on the theory by Bažant and enhanced by additional constitutive and thermodynamic relationships. A PC procedure has been included to check the exactness of the solution.

The study allows for estimating the durability performances of the tank: after about one month, all the structure is fully heated, possibly inducing thermal damage within concrete; such a result is slightly modified when modeling the domain more in detail, i.e. tank plus surrounding ground, or when changes in the salts level are considered. Even if at present some geometric and mechanical characteristics are still to be fixed and consequently they induce an unavoidable uncertainty on the numerical results, the generality of the approach is not affected by such restrictions, and the results can be evaluated just as first guidelines in defining design criteria for liquid salts concrete systems. In fact, this study is the first step in a new research field and will be extended within the Italian Research Project "Elioslab – Research Laboratory for Solar Technologies at High Temperatures" starting at the end of 2007.

Additionally, independently of the specificity and interest of the application, it has been shown here that the fully coupled mathematical-numerical model proposed

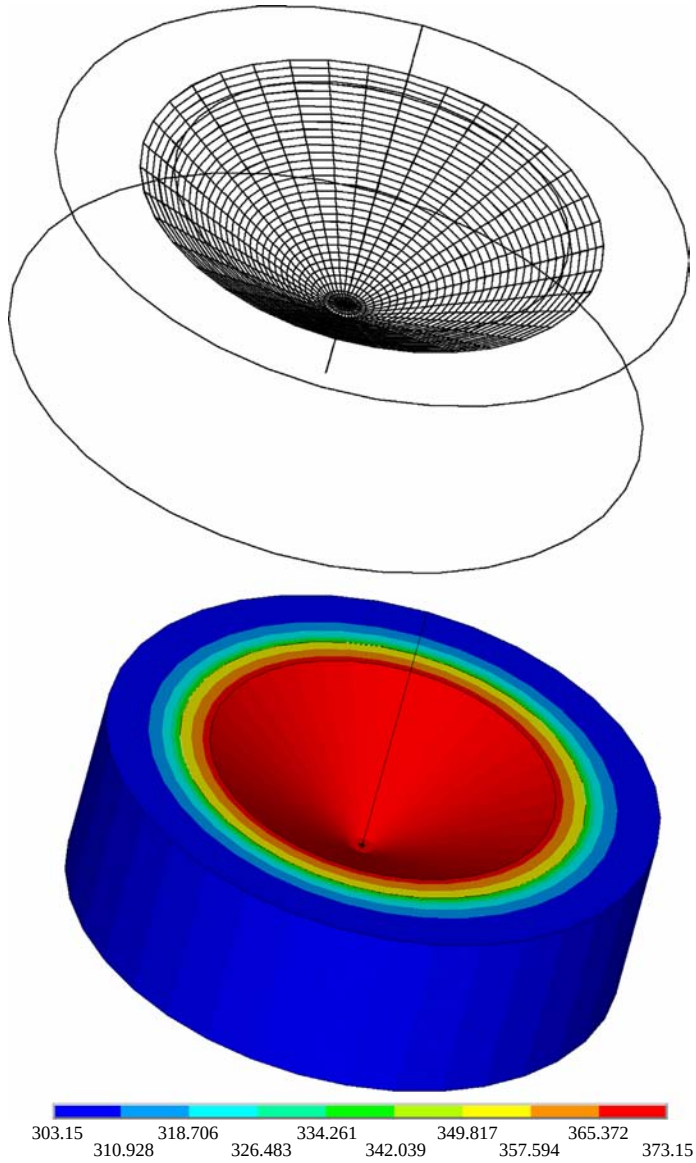

Figure 18.
Scheme of the whole domain and temperature distribution after five months

(whose details have been reported for the hygro-thermal field only and whose predictive abilities have already been demonstrated in Salomoni *et al.* (2007) even if in its not-upgraded form) has been enhanced through additional thermodynamic and constitutive relationships, allowing for obtaining more complete results in terms of water vapour pressure, gas pressure and capillary pressure which become fundamental variables mainly when higher temperature regimes are to be considered.

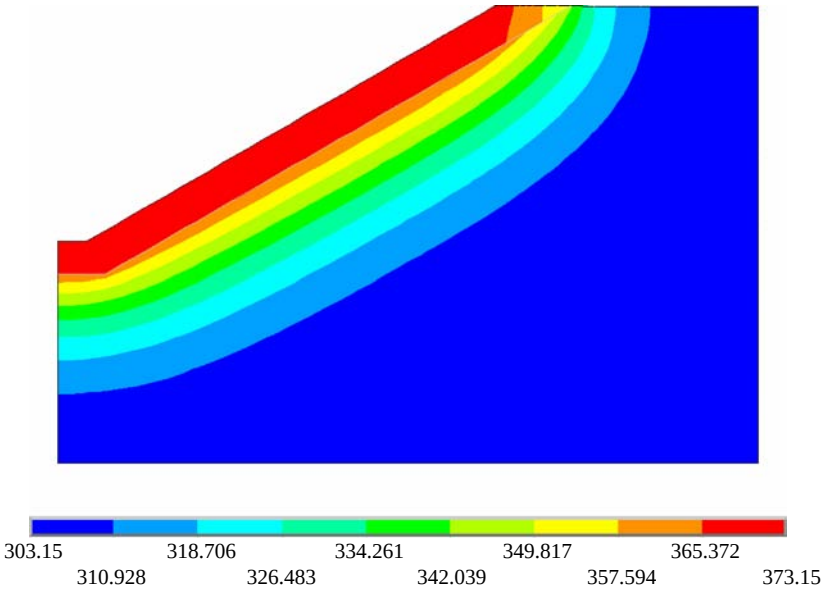

Figure 19.
Temperature distribution (K) after five months (section)

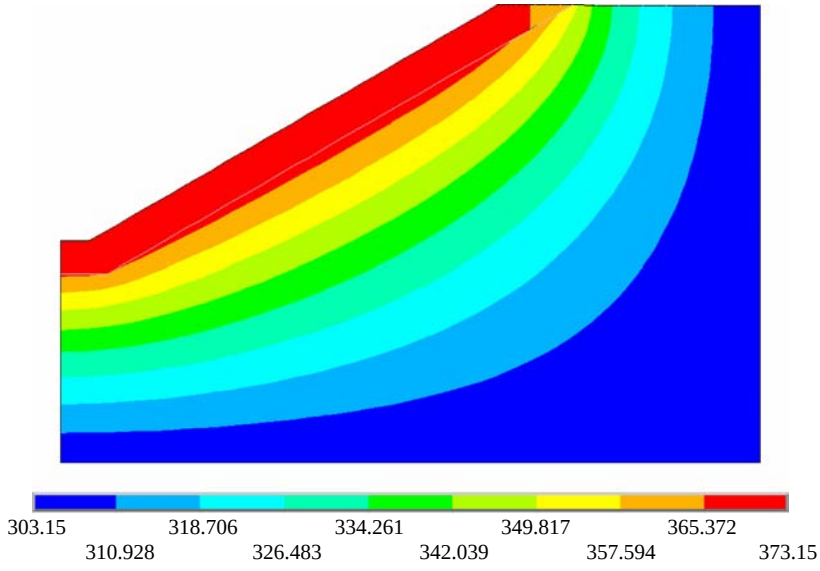

Figure 20.
Temperature distribution (K) after two years (section)

References

ASHRAE (1997), *Handbook of Fundamentals,* American Society of Heating, Refrigerating and Air Conditioning Engineers Inc., Atlanta, GA.

Baggio, P., Majorana, C.E. and Schrefler, B.A. (1995), "Thermo-hygro-mechanical analysis of concrete", *International Journal for Numerical Methods in Fluids*, Vol. 20, pp. 573-95.

Baroghel-Bouny, V., Mainguy, M., Lassabatere, T. and Coussy, O. (1999), "Characterization and identification of equilibrium and transfer moisture properties for ordinary and high-performance cementitious materials", *Cement and Concrete Research*, Vol. 29, pp. 1225-38.

Bažant, Z.P. (1975a), "Theory of creep and shrinkage in concrete structures: a précis of recent developments", in Nemat-Nasser, S. (Ed.), *Mechanics Today*, Vol. 2, Pergamon, New York, NY, pp. 1-93.

Bažant, Z.P. (1975b), "Pore pressure, uplift, and failure analysis of concrete dams", Int. Commission on Large Dams Symp. on Criteria and. Assumptions for Analysis of Dams Swansee.

Bažant, Z.P. (1986), "Material models for structural creep analysis", in Bažant, Z.P. (Ed.), *Creep and Shrinkage of Concrete: Mathematical Modeling, Ch. 2, Proc. of the 4th RILEM International Symposium, Northwestern University, Evanston, IL*.

Bažant, Z.P. (Ed.) (1988), *Mathematical Modelling of Creep and Shrinkage of Concrete*, Wiley, New York, NY.

Bažant, Z.P. and Najjar, L.N. (1971), "Drying of concrete as a non-linear diffusion problem", *Cement and Concrete Research*, Vol. 1, pp. 461-73.

Bažant, Z.P. and Najjar, L.N. (1972), "Nonlinear water diffusion in non-saturated concrete", *Materials and Structures*, Vol. 5 No. 25, pp. 3-21.

Bažant, Z.P. and Panula, L. (1979), "Practical prediction of time-dependent deformations of concrete", *Materials and Structures*, Vol. 12 No. 3, pp. 169-74.

Bažant, Z.P. and Thonguthai, W. (1978), "Pore pressure and drying of concrete at high temperature", *Journal of the Engineering Materials Division, ASME*, Vol. 104, pp. 1058-80.

Bažant, Z.P. and Thonguthai, W. (1979), "Pore pressure in heated concrete walls: theoretical predictions", *Magazine of Concrete Research*, Vol. 31 No. 107, pp. 67-76.

Bažant, Z.P. and Wittmann, F.H. (1982), *Creep and Shrinkage in Concrete Structures*, Wiley, New York, NY.

Bažant, Z.P., Chern, J.C., Rosenberg, A.M. and Gaidis, J.M. (1988), "Mathematical model for freeze-thaw durability of concrete", *Journal of the American Ceramic Society*, Vol. 71 No. 9, pp. 776-83.

Bear, J. (1988), *Dynamics of Fluids in Porous Media*, Dover, New York, NY.

Bentz, D.P., Garboczi, E.J. and Quenard, D.A. (1998), "Modelling drying shrinkage in reconstructed porous materials: application to porous Vycor glass", *Modelling and Simulation in Materials Science and Engineering*, Vol. 6 No. 3, pp. 211-36.

Cheng, H.P., Li, M.H. and Cheng, J.R. (2003), "An assessment of using the predictor-corrector technique to solve reactive transport equations", *International Journal for Numerical Methods in Engineering*, Vol. 56, pp. 739-66.

Chung, J.H. and Consolazio, G.R. (2005), "Numerical modeling of transport phenomena in reinforced concrete exposed to elevated temperatures", *Cement and Concrete Research*, Vol. 35 No. 3, pp. 597-608.

Chung, J.H., Consolazio, G.R. and McVay, M.C. (2006), "Finite element stress analysis of a reinforced high-strength concrete column in severe fires", *Computers & Structures*, Vol. 84, pp. 1338-52.

Copeland, R.J., West, R.E. and Kreith, F. (1984), "Thermal energy storage at 900°C", *Proc. of the 19th Ann. Intersoc. Energy Conversion Eng. Conf., San Francisco, 19-24 August*, pp. 1171-5.

Couture, F., Jomaa, W. and Ruiggali, J.R. (1996), "Relative permeability relations: a key factor for a drying model", *Transport in Porous Media*, Vol. 23, pp. 303-35.

ENEA (2007), available at: www.enea.it/com/ingl/solarframe.htm

England, G.L. and Ross, A.D. (1970), "Shrinkage, moisture and pore pressures in heated concrete", *Proc. of the American Concrete Institute – International Seminar of Concrete for Nuclear Reactors, Berlin*, pp. 883-907.

Forsyth, P.A. and Simpson, R.B. (1991), "A two-phase, two-component model for natural convection in a porous medium", *International Journal for Numerical Methods in Fluids*, Vol. 12, pp. 655-82.

Gawin, D., Majorana, C.E. and Schrefler, B.A. (1999), "Numerical analysis of hygro-thermal behaviour and damage of concrete at high temperature", *Mechanics of Cohesive-Frictional Materials*, Vol. 4, pp. 37-74.

Giannuzzi, G.M., Miliozzi, A., Majorana, C.E. and Salomoni, V. (2005), "Conceptual design of innovative heat storage systems for medium and high temperatures solar technology", *Proc. of TCN CAE 2005 – Int. Conf. on CAE and Computational Technologies for Industry, Lecce*, 5-8 October.

Giannuzzi, G.M., Majorana, C.E., Miliozzi, A., Salomoni, V.A. and Nicolini, D. (2007), "Structural design criteria for steel components of parabolic-trough solar concentrators", *ASME Journal of Solar Energy Engineering*, Vol. 129, pp. 382-90.

Goldschmit, M.B. and Cavaliere, M.A. (1997), "An iterative (*k-L*)-predictor/*(*-corrector algorithm for solving (*k-*() turbulent models", *Engineering Computations*, Vol. 14 No. 4, pp. 441-55.

Grasley, Z.C. and Lange, D.A. (2007), "Thermal dilation and internal relative humidity of hardened cement paste", *Materials and Structures*, Vol. 40, pp. 311-7.

Gregg, S.J. and Sing, K.S.W. (1982), *Adsorption, Surface Area and Porosity*, Academic Press, London.

Harmathy, T.Z. and Allen, L.W. (1973), "Thermal properties of selected masonry unit concretes", *ACI Journal*, Vol. 70 No. 15, pp. 135-42.

Herrmann, U., Kelly, B. and Price, H. (2004), "Two-tank molten salt storage for parabolic trough solar power plants", *Energy*, Vol. 29 Nos 5/6, pp. 883-93.

Hyland, R.W. and Wexler, A. (1983), "Formulation for the thermodynamic properties of dry air from 173.15K to 473.15K, and of saturated moist air from 173.15K to 372.15K, at pressures to 5MPa", *ASHRAE Transactions A*, Vol. 89 No. 2, pp. 520-35.

Ives, J., Newcomb, J.C. and Pard, A.G. (1985), "High temperature molten salt storage", SERI/STR-231-2836 (Technical paper).

Jayaraman, B. (1999), "Thermodynamic properties of air water mixtures (− 100 to 100°C and 50 to 5000 kPa)", *Air Conditioning and Refrigeration Journal*, April-June.

Ji, X. and Yan, J. (2006), "Thermodynamic properties for humid gases from 298 to 573K and up to 200 bar", *Applied Thermal Engineering*, Vol. 26, pp. 251-8.

Ji, X., Lu, X. and Yan, J. (2003), "Survey of experimental data and assessment of calculation methods of properties for the air-water mixture", *Applied Thermal Engineering*, Vol. 23, pp. 2213-28.

Khoury, G.A. and Majorana, C.E. (Eds) (2007), *Heat Effects on Concrete*, Thomas Telford, London.

Klinkenberg, L.J. (1941), "The permeability of porous media to liquids and gases", *Drilling and Production Practice*, American Petroleum Institute, Washington, DC, pp. 200-13.

Li, K. and Horne, R.N. (2001), "Gas slippage in two-phase flow and the effect of temperature", *SPE 68778, Proc. of the 2001 SPE Western Region Meeting, Bakersfield, CA, 26-30 March*.

Lüpfert, E., Geyer, M., Schiel, W., Esteban, A., Osuna, R., Zarza, E. and Nava, P. (2001), "EUROTROUGH design issues and prototype testing at PSA", *Proc. of ASME Int. Solar Energy Conference – Forum 2001, Solar Energy: The Power to Choose, Washington, DC, 21-25 April*, pp. 389-94.

McVay, M.C. and Rish, J.W. (1995), "Flow of nitrogen and superheated steam through cement mortar", *Journal of ThermoPhysics and Heat Transfer*, Vol. 9 No. 4, pp. 41-3.

Majorana, C.E. and Salomoni, V.A. (2004), "Parametric analyses of diffusion of activated sources in disposal forms", *Journal of Hazardous Materials*, Vol. A113, pp. 45-56.

Majorana, C.E., Salomoni, V. and Schrefler, B.A. (1998), "Hygrothermal and mechanical model of concrete at high temperature", *Materials and Structures*, Vol. 31, pp. 378-86.

Majorana, C.E., Salomoni, V. and Secchi, S. (1997), "Effects of mass growing on mechanical and hygrothermic response of three-dimensional bodies", *Journal of Materials Processing Technology*, Vol. 64 Nos 1/3, pp. 277-86.

Pilkington Solar International GmbH (2000), "Survey of thermal storage for parabolic-trough power plants", NREL/SR-550-27925 (Technical report).

Powers, T.C. and Brownyard, T.L. (1947), "Studies of the physical properties of hardened portland cement pastes", *Proc. Am. Concr. Inst., ACI Journal*, Vol. 41, pp. 845-80.

Price, H., Lupfert, E., Kearney, D., Zarza, E., Cohen, G., Gee, R. and Mahoney, R. (2002), "Advances in parabolic trough solar power technology", *ASME Journal of Solar Energy Engineering*, Vol. 124 No. 2, pp. 109-25.

Reid, R.C., Praunsnitz, J.M. and Bruce, E.P. (1987), *The Properties of Gases and Liquids*, McGraw-Hill, New York, NY.

Rubbia, C., and ENEA Working Group (2001), "Solar thermal energy production: guidelines and future programmes of ENEA", ENEA/TM/PRES/2001_7, Rome, (Technical report).

Salomoni, V.A. and Schrefler, B.A. (2005), "A CBS-type stabilizing algorithm for the consolidation of saturated porous media", *International Journal for Numerical Methods in Engineering*, Vol. 63, pp. 502-27.

Salomoni, V.A., Mazzucco, G. and Majorana, C.E. (2007), "Mechanical and durability behaviour of growing concrete structures", *Engineering Computations*, Vol. 24 No. 5, pp. 536-61.

Sargent & Lundy Consulting Group (2002), "Assessment of parabolic trough and power tower solar technology cost and performance forecasts", NREL SL-5641, Chicago, IL (Technical report).

Schrefler, B.A., Simoni, L. and Majorana, C.E. (1989), "A general model for the mechanics of saturated-unsaturated porous materials", *Materials and Structures*, Vol. 22, pp. 323-34.

Shazali, M.A., Baluch, M.H. and Al-Gadhib, A.H. (2006), "Predicting residual strength in unsaturated concrete exposed to sulphate attack", *Journal of Materials in Civil Engineering*, Vol. 18 No. 3, pp. 343-54.

Turska, E. and Schrefler, B.A. (1993), "On convergence conditions of partitioned solution procedures for consolidation problems", *Computer Methods in Applied Mechanics and Engineering*, Vol. 106, pp. 51-63.

Wylie, R.G. and Fisher, R.S. (1996), "Molecular interaction of water vapor and air", *Journal of Chemical & Engineering Data*, Vol. 41, pp. 133-42.

Zhukov, V.V. and Shevchenko, V.I. (1974), "Investigation of causes of possible spalling and failure of heat-resistant concretes at drying, first heating and cooling", in Nebrasov, K.D. (Ed.), *Zharostoikie Betony*, Stroiizdat, Moscow.

Corresponding author
Valentina A. Salomoni can be contacted at: salomoni@dic.unipd.it